Microporosity in Ordered Mesoporous Aluminosilicates Characterized by Catalytic Probing Reactions

Yinyong Sun, Yu Han, Lina Yuan, Shengqian Ma, Dazhen Jiang, and Feng-Shou Xiao*

Department of Chemistry & Key Laboratory of Inorganic Synthesis and Preparative Chemistry, Jilin University, Chang Chun 130023, China

Received: December 8, 2002

The microporosity of ordered mesoporous aluminosilicates assemblied from zeolite nanoclusters is investigated by catalytic reactions with various probing molecules. At first, the samples are treated by bulky basic organic molecular 5,7-dibrom-8-hydroxy-chinolin. In this case, the acidic sites in mesopores are killed, and the acidic sites in micropores that are smaller than the molecular diameter of 5,7-dibrom-8-hydroxy-chinolin are still active. The cracking of 1,3,5-triisopropylbenzene shows that the treated MAS-7 is still catalytically active. In contrast, the treated MAS-9 and treated Al-SBA-15 are almost inactive. These results show that MAS-7 contains micropores whose size is similar to that of beta. Furthermore, the catalytic cracking of cumene shows that the treated MAS-7 and treated MAS-9 are catalytically active but that the treated Al-SBA-15 is inactive. These results show that MAS-9 also contains micropores whose size is similar to that of ZSM-5. Additionally, the catalytic dehydration of 2-propanol (molecular diameter of 3.4 Å) shows that the treated MAS-7, treated MAS-9, and treated Al-SBA-15 are catalytically active. These results suggest that Al-SBA-15 also contains micropores that are larger than 3.4 Å, in good agreement with earlier reports.

1. Introduction

Since the M41S family of periodic mesoporous materials[1,2] was synthesized successfully by the assembly of cationic surfactants with inorganic precursors in the early 1990s, a number of investigations have been made of their structures and properties.[3−7] As a result, it was found that MCM-41 exhibited a hexagonal array of uniform channel mesopores and high surface area, but it showed poor hydrothermal stability.[8]

Some successful examples of increasing hydrothermal stability are disordered KIT-1,[9] wormlike disordered MSU-X,[10,11] and ordered hexagonal mesoporous SBA-15.[12] SBA-15 is usually prepared under strongly acidic conditions (pH < 1), and under strongly acidic conditions, it is very difficult to introduce heteroatoms into the framework of SBA-15. To solve this problem, much effort has been devoted to the incorporation of Al, Ti, and V into the framework of SBA-15, including "postsynthesis" grafting procedures[13−15] and "direct synthesis".[16,17] However, although the heteroatoms are introduced into SBA-15, they do not show as a high catalytic activity as they do in zeolites.

More recently, the pore structure of SBA-15 has been carefully investigated.[18−24] Davidson et al.[18] have reported the existence of a microporous corona around the mesopores of silica-based SBA-15 materials characterized by XRD, TEM, and N_2 adsorption; Ryoo and Jaroniec et al.[19,20] have reported a mesopore−micropore network in ordered mesopores of SBA-15 silica by TEM imaging of the inverse platinum replica and nitrogen adsorption. Inagaki et al.[21] have reported the control of the microporosity within the pore walls of ordered mesoporous silca SBA-15 by *t*-plots of nitrogen adsorption isotherms.

In our case, we have synthesized couples of ordered mesoporous aluminosilicates such as MAS-7[25] and MAS-9[26] assembled from zeolite beta and zeolite ZSM-5 nanoclusters with tricopolymer surfactants (P123), respectively, and these mesoporous aluminosilicates exhibited high hydrothermal stability and strong acidity as compared with those of Al-SBA-15. During the characterization of the pore structure of these mesoporous aluminosilicates by TEM and adsorption isotherms,[27] it was suggested that these ordered mesoporous aluminosilicates contain micropores, but it is difficult to characterize the micropore size in the mesoporous materials.[27]

However, catalytic reactions are very useful techniques for distinguishing porous structures because of the shape selectivity of reactants. In 1960, shape-selective catalysis was first reported by Weisz and Frilette,[28] and then many studies were reported on molecular shape-selective catalysis.[29−31] For example, Derouane[29] has reported on molecular shape-selective catalysis by zeolite ZSM-5. At the same time, the selective poisoning of acidic centers in a zeolite is also a very effective method for characterizing its porous structure and properties.[32−34]

In this paper, we characterize the microporosity in ordered mesoporous aluminosilicates of Al-SBA-15, MAS-7, and MAS-9 by using catalytic reactions of probing molecules with various diameters.

2. Materials and Methods

2.1. Materials. MAS-7 and MAS-9 were prepared according to the following procedure reported by Xiao and co-workers.[25,26] The typical synthesis for MAS-7 is as follows: (1) The zeolite precursors solution with zeolite beta primary structure units were prepared by adding 0.16 g of NaOH, 0.30 g of $NaAlO_2$, and 4.8 g of fumed silica to 25 mL of a TEAOH aqueous solution (20%) under stirring ($Al_2O_3/SiO_2/Na_2O$/TEAOH/H_2O molar ratios of 1.0/60/2.5/22/800) and then transferring the mixture into an autoclave for aging for 4 h at 413 K to get a clear solution. (2)EO20PO70EO20 (0.8 g, Pluronic P123) was dis-

* To whom correspondence should be addressed. E-mail: fsxiao@mail.jlu.edu.cn. Phone: +86-431-8922331-2314. Fax: +86-431-5671974.

10.1021/jp027656u CCC: $25.00
Published on Web 01/29/2003

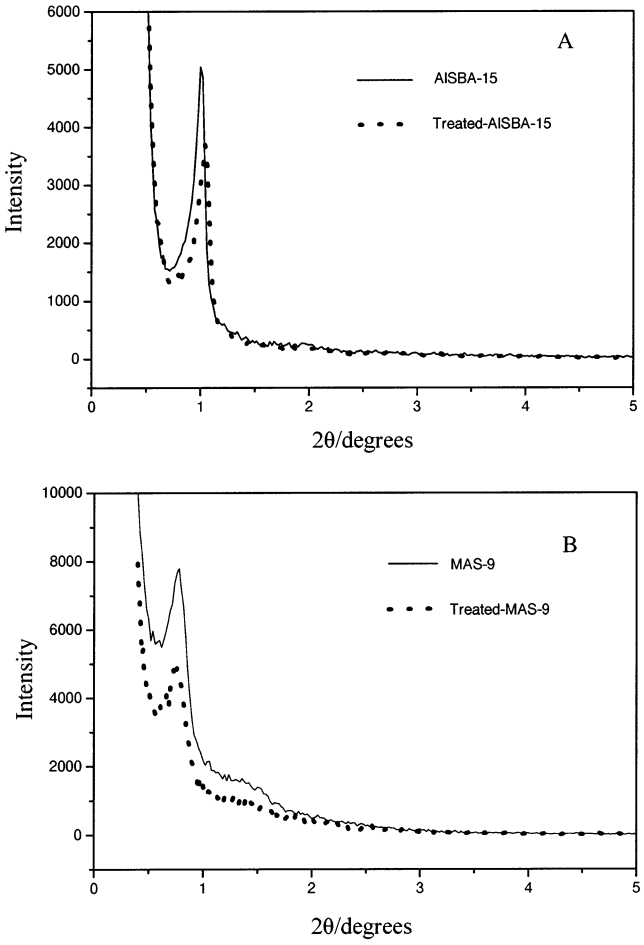

Figure 1. XRD patterns of (A) Al-SBA-15 and (B) MAS-9 without DBHC treatment (—) and with DBHC treatment (••).

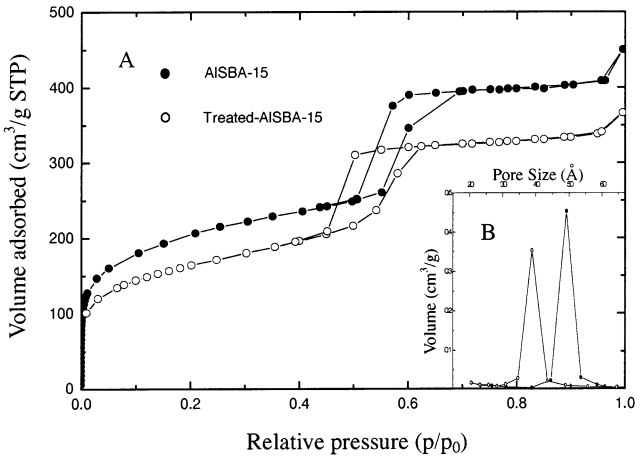

Figure 2. (A) Adsorption isotherms for N_2 and (B) mesopore size distribution of Al-SBA-15 without DBHC treatment (●) and with DBHC treatment (○).

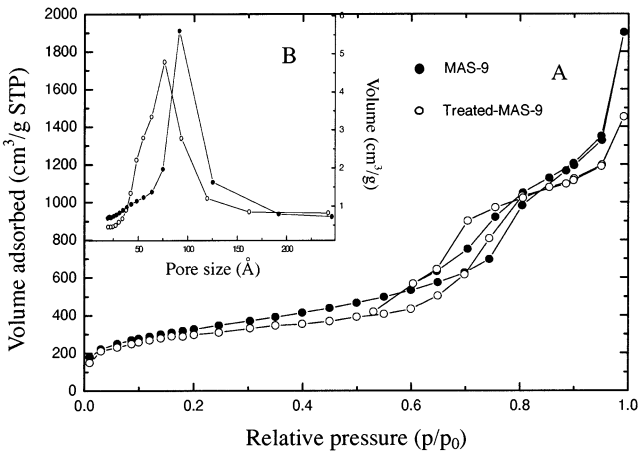

Figure 3. (A) Adsorption isotherms for N_2 and (B) mesopore size distribution of MAS-9 without DBHC treatment (●) and with DBHC treatment (○).

solved in 20 mL of H_2O mixed with 5 mL of HCl (10 M/L), followed by 2.5 mL of precursors solution (containing 8 mmol of SiO_2) obtained in step one. The mixture was stirred at 313 K for 20 h and then transferred into an autoclave for additional reaction at 373 K for 24 h. (3) The product (MAS-7) prepared from the aluminosilicate precursors was collected by filtration, dried in air, and calcined at 823 K for 5 h to remove the templates. MAS-9 is prepared according to the literature.[26]

For comparison, the Al-SBA-15 (synthetic temperature at 313 K),[16] beta,[35] and ZSM-5[36] samples are prepared according to the literature.

2.2. Materials Treatment. 5,7-Dibrom-8-hydroxy-chinolin (0.08 g, DBHC) was dissolved in 160 mL of anhydrous ethanol in a sealed container, and then 0.2 g of the sample was added to the solution under stirring. After stirring for 24 h at room temperature, the mixture was filtered, washed many times with anhydrous ethanol to remove excess DBHC, and dried for 20 h in an oven (373−393 K) under vacuum.

2.3. Measurements. X-ray powder diffraction patterns were performed on a Siemens D5005 instrument with Cu Kα radiation, a scanning speed of 2°/min, and scanning regions at 0.4−10° and 4−80°. The data of the BET surface area and the pore-size distribution of samples were measured on a Micromeritics ASAP 2010M system at 77 K using N_2 as an adsorbent, and the pore-size distributions for the mesopores and micropores were estimated by the Barrett−Joyner−Halenda (BJH) and Horvath−Kawazoe (HK) models, respectively.

2.4. Catalytic Reactions of Probing Molecules. The 2-propanol dehydration reaction was performed at 473 K by pulse injections. Cumene and 1,3,5-triisopropylbenzene (TIPB) cracking reactions were performed at 573 K by pulse injections. In each run, 50 mg of catalyst was used, the pulse injection of the reactant was 0.4 μL, and nitrogen was used as the carrier gas at a flow rate of 53.7 mL/min. The reaction products were analyzed by a Shimadzu GC-8A equipped with a TCD detector.

3. Results and Discussion

3.1. XRD and N_2 Adsorption. Figure 1 shows the XRD patterns of Al-SBA-15 (Si/Al = 20) and MAS-9 (Si/Al = 30) treated and untreated with DBHC molecules. Obviously, Al-SBA-15 and MAS-9 treated with DBHC molecules still exhibit their characteristic peaks assigned to hexagonal symmetry, but the XRD diffraction intensity is slightly reduced as compared to that of untreated samples, indicating that the samples treated with DBHC molecules basically keep their mesostructures.

Figures 2 and 3 show N_2 adsorption isotherms and pore distributions of Al-SBA-15 (Si/Al = 20) and MAS-9 (Si/Al = 30) treated and untreated with DBHC molecules, and the parameters for various samples are summarized in Table 1. The BET surface areas of Al-SBA-15, MAS-7, and MAS-9 without DBHC treatment are 752, 1183, and 980 m^2/g, respectively. However, after DBHC treatment, Al-SBA-15, MAS-7, and MAS-9 have surface areas of 580, 1001, and 820 m^2/g, respectively. Correspondingly, the mesopore sizes of Al-SBA-15, MAS-7, and MAS-9 are also reduced significantly, as

TABLE 1: Parameters of N_2 Adsorption Isotherms over Various Samples Treated and Untreated with DBHC Molecules

sample	surface area (m^2/g)	volume (cm^3/g)	pore size (Å)
Al-SBA-15	752	0.69	49
treated Al-SBA-15	580	0.49	38
MAS-7	980	1.34	82
treated MAS-7	820	1.12	70
MAS-9	1183	1.48	91
treated MAS-9	1001	1.19	76
beta	397	0.19	7.7
treated beta	391	0.19	7.7
ZSM-5	362	0.15	5.5
treated ZSM-5	359	0.15	5.5

TABLE 2: Molecular Kinetic Diameter of Reactants and DBHC

reagents	2-propanol	cumene	TIPB	DBHC
kinetic diameter	3.4 Å	5.0 Å	7.4 Å	8.7 Å

TABLE 3: Catalytic Activities of Various Samples without Treatment of DBHC Molecules

	conversion (%)		
catalyst (Si/Al)	2-propanol dehydration	cumene cracking	1,3,5-triisopropylbenzene (TIPB) cracking
ZSM-5 (30)	100	90.1	4.5
beta (30)	100	93.4	100
Al-SBA-15 (30)	100	12.5	92.5
Al-SBA-15 (20)	100	33.2	98.4
MAS-7 (30)	100	30.4	97.3
MAS-9 (30)	100	29.5	95.1

observed in Table 1. These results indicate that the DBHC molecules really enter into the mesopores of mesoporous materials. In contrast, ZSM-5 and beta treated and untreated with DBHC molecules show almost the same surface area and pore size. These results confirm that DBHC molecules cannot enter into the micropores of zeolites.

3.2. Catalytic Reactions and Reactant Diameters. Catalytic reactions of probing molecules include the 2-propanol dehydration and cracking of cumene and TIPB. It is well known that the 2-propanol dehydration is a typical weak acid-catalyzed reaction and that molecular cracking is typical strong acid-catalyzed reaction.[37]

The kinetic diameters of probing molecules in these catalytic reactions and DBHC are presented in Table 2. Notably, the molecular diameters of 2-propanol, cumene, TIPB, and DBHC are 3.4, 5.0, 7.4, and 8.7 Å, respectively.[38] If the acidic samples are treated by basic molecule DBHC, then the acidic sites in the pores larger than 8.7 Å will be killed and the acidic sites in the pores smaller than 8.7 Å will still be active. Then we can test their catalytic activity by using probing molecules smaller than DBHC to judge what kind of micropores these samples contain.

3.3. Catalytic Activities of Various Samples without Treatment by DBHC. Catalytic activities of various samples without treatment by DBHC are shown in Table 3. In 2-propanol dehydration, ZSM-5, beta, Al-SBA-15, MAS-7, and MAS-9 show very high activity, having near 100% conversion. These results indicate that both microporous zeolites and mesoporous aluminosilicates are good catalysts for 2-propanol dehydration.

In cumene cracking, microporous zeolites of ZSM-5 and beta exhibit high activity at 90.1 and 93.4%, respectively. In contrast, the mesoporous aluminosilicates of Al-SBA-15, MAS-7, and MAS-9 show relatively low conversions of 12.5−30.4%. The big difference in catalytic acitivities over microporous zeolites and mesoporous aluminosilicates may result from their distinguishable acidic strengths. Furthermore, we find that MAS-7 and MAS-9 (conversions of 30.4 and 29.5%, respectively) are more active than Al-SBA-15 (conversion of 12.5%) under the same Si/Al ratio, indicating that the acidic strengths of MAS-7 and MAS-9 are much stronger than that of Al-SBA-15.

TABLE 4: Catalytic Activities of Various Samples with Treatment of DBHC Molecules

	conversion (%)		
catalyst (Si/Al)	2-propanol dehydration	cumene cracking	1,3,5-triisopropylbenzene cracking
ZSM-5 (30)	100	89.2	[a]
beta (30)	100	92.7	100
Al-SBA-15 (30)	41.1	[a]	[a]
Al-SBA-15 (20)	100	[a]	[a]
MAS-7 (30)	81.1	3.5	12.5
MAS-9 (30)	79.2	3.2	[a]

[a] Undetectable.

In TIPB cracking, the samples of beta, Al-SBA-15, MAS-7, and MAS-9 show high activity, with conversions of 100, 92, 97, and 95%, respectively. However, ZSM-5 shows relatively low catalytic activity, with a conversion of 4.5%. These results are assigned to the following reasons (1) The reactant molecule of TIPB cannot enter the pores of ZSM-5 because the pore size of ZSM-5 is only about 5.5 Å and the TIPB dimension is near 7.4 Å. (2) The catalytic activity is contributed from the few acidic sites on the external surface.

3.4. Catalytic Activities of Various Samples Treated by DBHC. Catalytic activities of various samples treated by DBHC are presented in Table 4. In the catalytic cracking of the large molecule TIPB, the treated ZSM-5 is completely inactive, which is attributed to the fact that the acidic sites of ZSM-5 on the external surface are poisoned and the probing molecule of TIPB (7.4 Å) cannot enter its pore (5.5 Å). The treated beta still shows high activity (conversion near 100%), which is attributed to the fact that the acidic sites of beta zeolite are mostly located in the internal surface and DBHC (8.7 Å) cannot enter its pores (7.7 Å) to kill its acidic sites in the internal surface, but the probing molecule of TIPB (7.4 Å) can easily enter its pores, reacting with the acidic sites in the internal surface. However, the treated Al-SBA-15 (Si/Al = 20 and 30) samples are inactive, suggesting that the acidic sites in the pores larger than 8.7 Å are killed and that there are no micropores with sizes between 7.4 and 8.7 Å. However, the treated MAS-7 still shows a conversion of 12.5%, suggesting that there are micropores with sizes between 7.4 and 8.7 Å in the sample of MAS-7 because the acidic sites in the pores larger than 8.7 Å are killed by the DBHC molecule and the TIPB molecule cannot touch the acidic sites in micropores with sizes less than 7.4 Å. Considering that the pore size of zeolite beta is about at 7.7 Å, we propose that the micropores with sizes between 7.4 and 8.7 Å are introduced by zeolite beta nanoclusters used in the synthesis. Additionally, we find that the treated MAS-9 is also inactive, suggesting that there are no micropores with sizes between 7.4 and 8.7 Å in the sample of MAS-9.

In the catalytic cracking of the small molecule cumene, the treated ZSM-5 shows a high conversion of 89.2%, which is a little lower than that of untreated ZSM-5 (90.1%) because its few acidic sites on the external surface are killed by the DBHC molecule and the internal acidic sites are unaffected. These results indicate that the acidic sites in the internal surface play a major role in cumene cracking. The treated beta also shows high activity (conversion of 92.7%), which is a little lower than that of untreated beta (93.4%) because its few acidic sites on

the external surface are killed. Furthermore, we observe that the treated Al-SBA-15 (Si/Al = 20 and 30) samples are inactive. Considering the fact the acidic sites in the pores larger than 8.7 Å are killed by the DBHC molecule, it is suggested that there are no micropores with sizes between 5.0 and 8.7 Å in Al-SBA-15. However, the treated MAS-7 and MAS-9 samples show conversions of 3.5 and 3.2%, respectively, suggesting that the two samples contain micropores with sizes between 5.0 and 8.7 Å. Because MAS-9 is inactive for TIPB cracking, we conclude that the microporous size of MAS-9 should be at 5.0−7.4 Å, which is consistent with that of the ZSM-5 (5.4 × 5.5 Å) nanoprecursors used for MAS-9.

In the catalytic dehydration of 2-propanol, the treated zeolites of ZSM-5 and beta still show high activity (conversion of 100%) because their mostly acidic sites are not killed and probing molecules of 2-propanol (3.4 Å) easily enter their micropores. Additionally, the treated mesoporous aluminosilicates of Al-SBA-15, MAS-7, and MAS-9 also show high activity (conversion of 41−100%), indicating that these mesoporous aluminosilicates contain micropores in the range of 3.4−8.7 Å. By considering the fact that the treated Al-SBA-15 is completely inactive for cumene and TIPB cracking, it is suggested that the microporous size in Al-SBA-15 is 3.4−5.0 Å, which is in good agreement with ealier reports.[21]

By summarizing the catalytic data over the treated samples, it is very interesting that the microporous size of these mesoporous aluminosilicates is distinguishable. For example, Al-SBA-15 contains micropores with sizes of 3.4−5.0 Å; MAS-9 contains micropores with sizes of 5.0−7.4 Å; and MAS-7 contains micropores with sizes of 7.4−8.7 Å. Obviously, the microporous size of mesoporous aluminosilicates could be controlled by the synthetic conditions.

In previous reports,[18−21] it has been reported that SBA-15 contains micropores that arise from the partial occlusion of the PEO chains in the aluminosilicate matrix, which become microporous upon calcination. However, it is difficult to characterize the microporous size in Al-SBA-15. In this paper, by using the catalytic dehydration of 2-propanol, we have directly obtained evidence that Al-SBA-15 contains micropores with sizes of 3.4−5.0 Å.

The preparations of MAS-7 and MAS-9 were assemblied from zeolite nanoclusters (zeolite structural units) of beta and ZSM-5, respectively. The existence of zeolite nanoclusters[39−41] (zeolite structural units) may be a key factor in the control of microporous structure. It has been reported that the micropore size of beta zeolite is about 6.6 × 7.7 Å and that the micropore size of ZSM-5 zeolite is about 5.4 × 5.5 Å.[42] Accordingly, catalytic data in the cracking of cumene and TIPB show that MAS-7 and MAS-9 assemblied from beta and ZSM-5 nanoclusters contain micropores with sizes of 7.4−8.7 Å and 5.0−7.4 Å, respectively. Significantly, the micropore size of mesoporous aluminosilicates assemblied from zeolite nanoclusters could be controlled by the use of various types of zeolite nanoclusters. Although our results show distinguishable micropores in MAS-7, MAS-9, and Al-SBA-15, we believe that in MAS-7 and MAS-9 there are also micropores resulting from the partial occlusion of the PEO chains to the aluminosilicate matrix, just like those in Al-SBA-15. More recently, the HRTEM technique[27] showed the direct observation of the micropores within these mesoporous aluminosilicates, and nanorange-ordered microporosity is found within the mesopore walls of MAS-7 and MAS-9. Liu et al.[27] proposed that nanorange-ordered microporosity results from zeolite primary structural units, in good agreement with our results, which might be the key to the high hydrothermal stability of MAS-7 and MAS-9.

Conclusions

Ordered mesoporous aluminosilicates of Al-SBA-15, MAS-7, and MAS-9 are treated by a bulky basic organic molecule (5,7-dibrom-8-hydroxy-chinolin, DBHC), and the acidic sites in mesopores are killed. Catalytic reactions including the cracking of 1,3,5-triisopropylbenzene (TIPB) and cumene and the dehydration of 2-propanol directly show that the micropore sizes of Al-SBA-15, MAS-7, and MAS-9 are distinguishable. The treated Al-SBA-15 is catalytically active for 2-propanol dehydration but not for the cracking of cumene and TIPB; the treated MAS-9 is catalytically active for 2-propanol dehydration and cumene cracking but not for TIPB cracking; the treated MAS-7 is catalytically active for 2-propanol dehydration and the cracking of cumene and TIPB. The catalytic data show that Al-SBA-15 contains micropores with sizes of 3.4−5.0 Å; MAS-9 contains micropores with sizes of 5.0−7.4 Å; MAS-7 contain micropores with sizes of 7.4−8.7 Å.

Acknowledgment. This work was supported by the National Natural Science Foundation of China (29825108, 20173022, and 20121103) and the State Basic Research Project (grant number G2000077507).

References and Notes

(1) Kresge, C. T.; Leonowicz, M. E.; Vartuli, J. C.; Beck, J. S. *Nature (London)* **1992**, *359*, 710.
(2) Beck, J. S.; Vartuli, J. C.; Roth, W. J.; Leonowica, M. E.; Kresge, C. T.; Schmitt, K. D.; Chu, C. T.-W.; Olson, D. H.; Sheppard, E. W.; MCCullen, S. B.; Higgins, J. B.; Schlenkler, J. L. *J. Am. Chem. Soc.* **1992**, *112*, 10834.
(3) Sayari, A.; Liu, P.; Kruk, M.; Jaroniec, M. *Chem. Mater.* **1997**, *9*, 2499.
(4) Long, Y. C.; Xu, T. M.; Sun, Y. J.; Dong, W. Y. *Langmuir* **1998**, *14*, 6173.
(5) Kruk, M.; Jaroniec, M.; Sayari, A. *Chem. Mater.* **1999**, *11*, 492.
(6) Jaroniec, M.; Kruk, M.; Olivier, J. P. *Langmuir* **1999**, *15*, 5410.
(7) Biz, S.; Occelli, M. L. *Catal. Rev.—Sci. Eng.* **1998**, *40*, 329.
(8) Corma, A. *Chem. Rev.* **1997**, *97*, 2373.
(9) Kim, J. M.; Jun, S.; Ryoo, R. *J. Phys. Chem. B* **1999**, *103*, 6200.
(10) Bagshaw, S. A.; Prouzet, E.; Pinnavaia, T. J. *Science (Washington, D.C.)* **1995**, *269*, 1242.
(11) Bagshaw, S. A.; Pinnavaia, T. J. *Angew. Chem., Int. Ed. Engl.* **1996**, *35*, 1102.
(12) Zhao, D.; Feng, J.; Huo, Q.; Melosh, N.; Fredrickson, G.; Chmelks, B.; Stucky, G. D. *Science (Washington, D.C.)* **1998**, *279*, 548.
(13) Luan, Z.; Hartmann, M.; Zhao, D.; Zhou, W.; Kevan, L. *Chem. Mater.* **1999**, *11*, 1621.
(14) Morey, M. S.; O'Bren, S.; Schwarz, S.; Stucky, G. D. *Chem. Mater.* **2000**, *12*, 898.
(15) Luan, Z.; Bae, J. Y.; Kevan, C. *Chem. Mater.* **2000**, *12*, 3202.
(16) Yue, Y.; Cedeon, A.; Bonardet, J.-L.; Melosh, N.; D'Esinose, J.-B.; Fraissard, J. *Chem. Commun.* **1999**, *109*, 1697.
(17) Bharat, L. N.; Johnson, O.; Sridhar, K. *Chem. Mater.* **2001**, *13*, 552.
(18) Imperor-Clerc, M.; Davidson, P.; Davidson, A. *J. Am. Chem. Soc.* **2000**, *122*, 11925.
(19) Kruk, M.; Jaroniec, M.; Ko, C. H.; Ryoo, R. *Chem. Mater.* **2000**, *12*, 1961.
(20) Ryoo, R.; Ko, C. H.; Kruk, M.; Antochshuk, V.; Jaroniec, M. *J. Phys. Chem. B* **2000**, *104*, 11465.
(21) Miyazawa, K.; Inagaki, S. *Chem. Commun.* **2000**, 2121.
(22) Zhao, D.; Huo, Q.; Feng, J.; Chmelka, B. F.; Stucky, G. D. *J. Am. Chem. Soc.* **1998**, *120*, 6024.
(23) Lukens, W. W., Jr.; Schmidt-Winkel, P.; Zhao, D.; Feng, J.; Stucky, G. D. *Langmuir* **1999**, *15*, 5403.
(24) Ravikovitch, P. I.; Neimark, A. V. *J. Phys. Chem. B* **2001**, *105*, 6817.
(25) Han, Y.; Xiao, F.-S.; Wu, S.; Sun, Y. Y.; Meng, X. J.; Li, D. S.; Lin, S.; Deng, F.; Ai, X. J. *J. Phys. Chem. B* **2001**, *105*, 7963.

(26) Han, Y.; Wu, S.; Sun, Y. Y.; Li, D. S.; Xiao, F.-S.; Liu, J.; Zhang, X. Z. *Chem. Mater.* **2002**, *14*, 1144.
(27) Liu, J.; Zhang, X.; Han, Y.; Xiao, F.-S. *Chem. Mater.* **2002**, *14*, 2536.
(28) Weisz, P. B.; Frilette, V. J. *J. Phys. Chem.* **1960**, *64*, 382.
(29) Derouane, E. G. *Stud. Surf. Sci. Catal.* **1980**, *5*, 5.
(30) Csicsery, S. M. In *Zeolite Chemistry and Catalysis*; Rabo, J. A.; Ed.; ACS Monograph No.171; American Chemical Society: Washington, DC, 1976; p 680.
(31) Weisz, P. B. In *Proc. 7th Inter. Congress Catal.*, Tokyo, Japan, 1980.
(32) Huang, C. P.; Richardaon, J. T. *J. Catal.* **1977**, *57*, 332.
(33) Forni, P. *Catal. Rev.* **1973**, *8*, 69.
(34) Fejes, P.; Kiricsi, I.; Hannus, I.; Tihanyi, T.; Kiss, A. *Stud. Surf. Sci. Catal.* **1980**, *5*, 135.
(35) Song, T.; Liu, L.; Xu, R. *Cuihua Xuebao* **1991**, *12*, 283.
(36) Zhou, Q.; Pang, W.; Qiu, S.; Jia, M. CN Patent ZL 93 1 17593.3, 1996. Zhou, Q.; Li, B.; Qiu, S.; Pang, W. *Chem. J. Chin. Univ.* **1999**, *20*, 693.
(37) Yue, Y. H.; Sun, Y.; Xu, Q.; Gao, Z. *Appl. Catal., A* **1998**, *175*, 131.
(38) *Cerius*^{2}*;* Molecular Simulation/Biosysm Corporation: San Diego, CA, 1995.
(39) Zhang, Z.; Han, Y.; Zhu, L.; Wang, R.; Yu, Y.; Qiu, S.; Zhao, D.; Xiao, F.-S. *Angew. Chem., Int. Ed.* **2001**, *40*, 1258.
(40) Liu, Y.; Zhang, W.; Pinnavaia, T. J. *J. Am. Chem. Soc.* **2000**, *122*, 8791.
(41) Trong On, D.; Kaliaguine, S. *Angew. Chem., Int. Ed.* **2001**, *40*, 3248.
(42) *Atlas of Zeolite Framework Types*, 5th ed.; Baerlocher, Ch., Meier, W. M., Olson, D. H., Eds.; Elsevier: Amsterdam, 2001.